High viral abundance and low diversity are associated with increased CRISPR-Cas prevalence across microbial ecosystems

S. Meaden[1,2¶#], A. Biswas[2, 3¶], K. Arkhipova[4], S. E. Morales[2*], B. E. Dutilh[4*], E. R. Westra[1*], P. C. Fineran[2,5*]

1. *Biosciences, University of Exeter, Penryn, TR10 9EZ, UK*
2. *Department of Microbiology and Immunology, University of Otago, PO Box 56, Dunedin 9054, New Zealand*
3. *Grasslands Research Centre, AgResearch, PO Box 11008, Palmerston North, 4442, New Zealand*
4. *Theoretical Biology and Bioinformatics, Science for Life, Utrecht University, Utrecht, the Netherlands*
5. *Bio-Protection Research Centre, University of Otago, PO Box 56, Dunedin 9054, New Zealand*

¶*These authors contributed equally to this work*

**These authors share senior authorship*

#Correspondence: Sean Meaden; S.Meaden@exeter.ac.uk

Keywords: CRISPR-Cas; bacteriophages; metagenomics; microbial ecology

Abstract

CRISPR-Cas are adaptive immune systems that protect their hosts against viruses and other parasitic mobile genetic elements. Consequently, selection from viruses and other genetic parasites is often assumed to drive the acquisition and maintenance of these immune systems in nature, but this remains untested. Here, we analyse the abundance of CRISPR arrays in natural environments using metagenomic datasets from 332 terrestrial, aquatic and host-associated ecosystems. For each metagenome we quantified viral abundance and levels of viral community diversity to test whether these variables can explain variation in CRISPR-Cas abundance across ecosystems. We find a strong positive correlation between CRISPR-Cas abundance and viral abundance. In addition, when controlling for differences in viral abundance, we found that the CRISPR-Cas systems are more abundant when viral diversity is low. We also found differences in relative CRISPR-Cas abundance among environments, with environmental classification explaining ~24% of variation in CRISPR-Cas abundance. However, the correlations with viral abundance and diversity are broadly consistent across diverse natural environments. These results indicate that viral abundance and diversity are major ecological factors that drive the selection and maintenance of CRISPR-Cas in microbial ecosystems.

Significance statement

Numerous studies demonstrate that CRISPR-Cas immune systems can provide defence against bacteriophage and archaeal viruses, yet little is known about the ecological conditions where CRISPR-Cas immunity is favoured. Moreover, our knowledge is largely confined to laboratory studies and it is unknown if viruses are a key selective driver of CRISPR-Cas in nature. Using metagenomic data from diverse environments we find that both viral abundance and the abundance of CRISPR-Cas immune systems correlate positively across most environments. Furthermore, CRISPR-Cas systems are more prevalent when viral diversity is low. These results extend previous theoretical work by demonstrating that viruses are a key driver of selection of CRISPR-Cas immune systems across many natural ecosystems.

Introduction

CRISPR-Cas is a sophisticated immune system of bacteria and archaea that is widespread across diverse prokaryotic taxa [1]. Anecdotal evidence suggests that CRISPR-Cas systems are unevenly distributed across environments and species. For example, culturable bacteria seem to have higher frequencies of CRISPR-Cas than non-culturable lineages [2], and extremophiles tend to have higher CRISPR-Cas content and longer CRISPR arrays than mesophiles [3, 4]. Given that CRISPR-Cas, like most defence system genes, are frequently lost and gained, this strongly suggests that CRISPR-Cas is advantageous under particular environmental conditions [5]. However, environmental parameters that determine the benefits of CRISPR-Cas remain unclear. *In vitro* studies suggest that the density of phages is a key fitness determinant of CRISPR-Cas immune systems [6], as high phage density favours the evolution of surface-based resistance over CRISPR-Cas. However, whether phage density explains the distribution of CRISPR-Cas in natural environments remains unexplored. Moreover, theory and laboratory experiments suggest that environments with genetically diverse phage populations may favour organisms with generalist defences over those containing the specific CRISPR-Cas system [7].

While these questions have been explored using theory and controlled laboratory-based experiments, they are rarely assessed using environmental samples [8–11]. The increasing availability of metagenomic data from a range of environments now provides an opportunity to test these hypotheses. Here, we quantify CRISPR array abundance and diversity across metagenomic samples that span a range of terrestrial, aquatic and host-associated ecosystems. We combine these data with measures of viral abundance and diversity to test to what extent these variables explain the distribution of CRISPR-Cas systems in natural environments. Across different types of environments, we consistently find a positive correlation between CRISPR-Cas abundance and viral abundance and a negative correlation with viral diversity. Taken together, these results imply that CRISPR-Cas is most beneficial in environments with high viral abundance but low diversity and that these are important drivers of the prevalence of CRISPR-Cas immune systems in the environment.

Results

Variation in CRISPR-Cas abundance is partially explained by viral abundance

While it is well-established that CRISPR-Cas immune systems can protect bacteria and archaea against viral infections under *in vitro* laboratory conditions, it remains unclear how important these genetic parasites are as a selective force for the maintenance of CRISPR-Cas systems in nature [12]. To assess the role of viruses as a selective force for CRISPR-Cas, we first compiled a dataset of 332 metagenomes and quantified the abundance of CRISPR-Cas systems and viruses in each sample. We note that our analyses uses all contigs classified as viral, and while the vast majority of these are of bacteriophage origin, we refer to these simply as viral for consistency (benchmarking analyses of our classifier vs. existing tools is available in the SI). These metagenomes vary in both CRISPR-Cas and viral abundance and therefore, provided a suitable dataset to test the hypothesis that viral abundance drives selection for CRISPR-Cas (Fig. 1). We found a positive correlation between viral abundance and the abundance of CRISPR-Cas systems (GLM, $F_{1,295} = 77.78$, $p < 0.0001$, Fig. 1), with viral abundance explaining around 20% of the observed variation in CRISPR-Cas abundance ($R^2 = 0.209$). We obtained qualitatively the same result when we included archaeal abundance in our model, which typically carry more CRISPR-Cas immune systems than bacteria [1]. These results strongly suggest that viruses are a fundamental selective force for the maintenance of CRISPR-Cas across diverse environmental conditions.

125

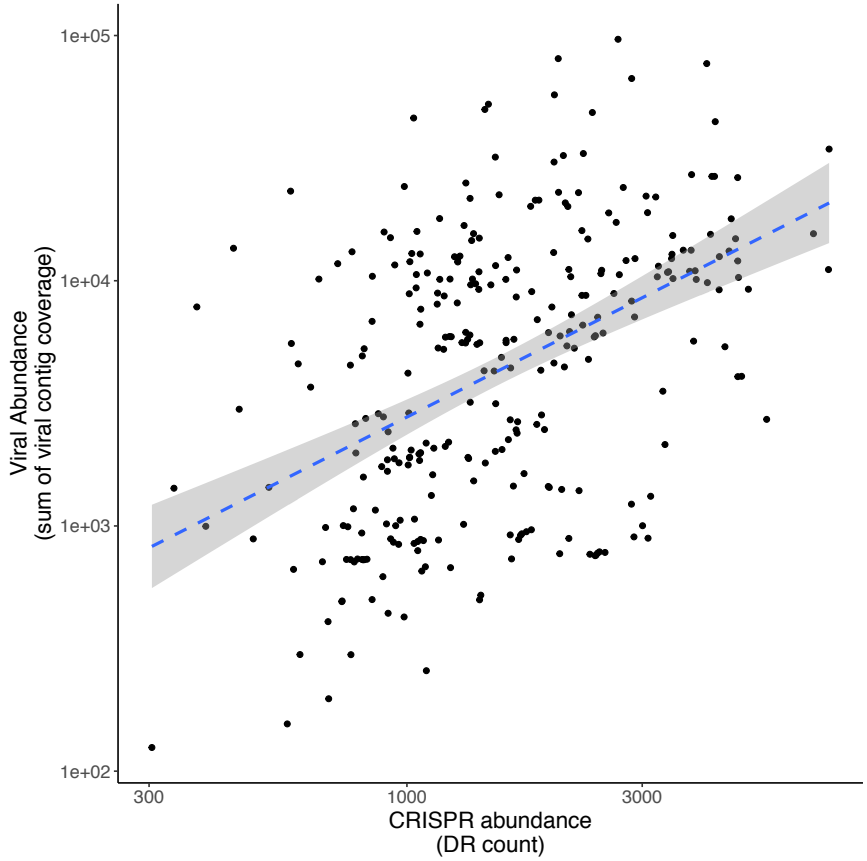

126 **Figure 1. CRISPR abundance positively correlates with viral abundance.**
127 Correlation between relative viral abundance and the read count (per million) of metagenomic reads
128 that mapped to CRISPR array repeats across all samples. The dashed line represents the linear
129 model fit and shaded area represents 95% confidence interval (p-value < 0.0001 and R^2 = 0.21).
130

131 ***Environmental conditions influence CRISPR-Cas abundance***

132 In addition to viruses being a selective force for CRISPR-Cas, ecological factors may
133 determine when CRISPR-Cas is beneficial and therefore, CRISPR-Cas abundance
134 may vary across different natural environments [13]. We therefore grouped samples
135 into ecologically meaningful categories, using the Earth Microbiome Project's sample
136 ontology (EMPO). This framework is structured to capture two major environmental
137 axes on which bacterial community composition orient, namely host-association and
138 salinity [14]. Level 1 of the ontology classifies samples as host-associated or free
139 living, level 2 classifies samples as saline or non-saline, or animal or plant-
140 associated and level 3 describes microbial environments that can be grouped into
141 levels 1 and 2 hierarchically (Fig. 2A [14]). These EMPO classifications highlighted
142 the varied CRISPR-Cas and viral abundance in these different environments (Fig. 2
143 and Fig. S2). Using this EMPO classification, we observed substantial variation in

CRISPR-Cas abundance, both within and between environment types (Fig. 2). For example, host-associated communities had a greater prevalence of CRISPR-Cas than free-living environments (GLM, $F_{1,330} = 7.01$, $p = 0.008$), although this classification only explained around 2% of the variation in CRISPR-Cas abundance. In contrast, more fine scaled classification of environments (such as gut, saline sediment etc. as per EMPO level 3 classification, Fig. 2C), explained 24% of the variation in CRISPR-Cas abundance. Taken together, these results suggest that in addition to viruses as a key selective force for the maintenance of CRISPR-Cas, there are substantial differences in CRISPR-Cas abundance among natural environments.

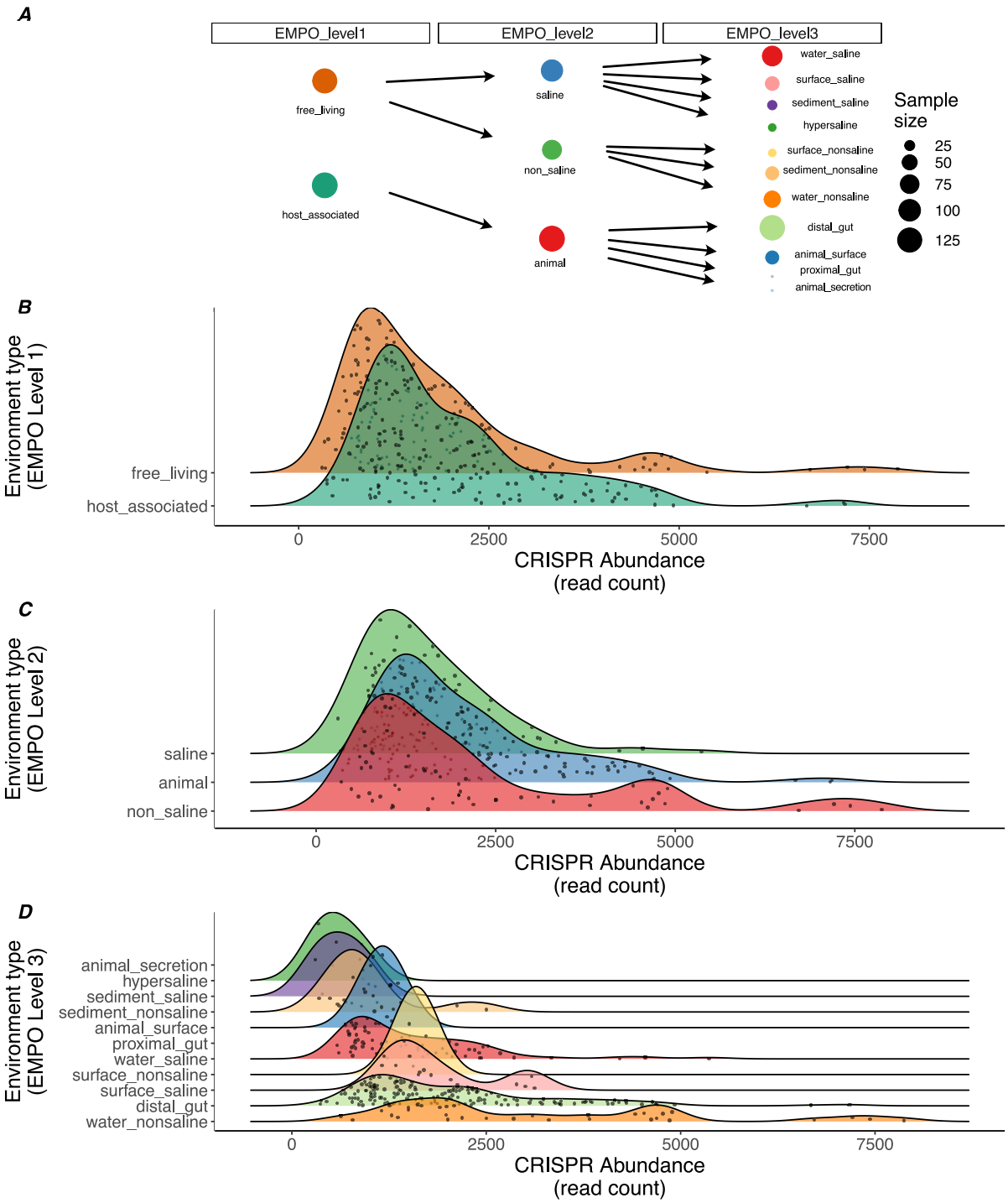

Figure 2. CRISPR abundance varies by environment. Distributions of metagenomic read counts that mapped to CRISPR arrays (read count per million that mapped to a CRISPR array predicted by CRISPRDetect v.3 from assembled contigs) grouped by environmental classification. (A) Sample sizes and ontology is shown in panel A. Samples are grouped using the Earth Microbiome Project Ontology (EMPO) at level 1 (B), 2 (C) or 3 (D).

164 ***Microbial community composition explains some variation in CRISPR-Cas***
165 ***abundance***
166 Although we found effects of viral abundance and environmental classification on
167 CRISPR-Cas abundance, it is plausible that these effects may be driven by
168 differences in the microbial community composition as CRISPR-Cas prevalence can
169 differ among taxa [1, 2]. We examined whether the variation in CRISPR-Cas
170 abundance across these metagenomes might be affected microbial community
171 composition. We found a weak but significant relationship between CRISPR-Cas
172 abundance and class-level community composition (PERMANOVA, $F_{1, 313} = 12.4$, p
173 < 0.001, $R^2 = 0.04$, permutations = 9999, distance metric = Bray-Curtis). We next
174 used clustering analyses to assess how well the EMPO framework levels grouped
175 our samples based on community composition and extracted the taxa that best
176 described differences among samples (Fig. S3A). In addition, we fitted CRISPR-Cas
177 abundance to this ordination to identify 'hotspots' of samples enriched with CRISPR-
178 Cas (Fig. S3B). With this approach, we identified multiple groups of samples with
179 high CRISPR-Cas abundance, supporting the notion that microbial phylogeny alone
180 only explains a limited amount of variation in CRISPR-Cas abundance. Additional
181 factors may contribute to the differences in CRISPR-Cas abundance across
182 environment types. Furthermore, high rates of horizontal gene transfer (HGT) across
183 taxa, coupled with frequent gain or loss of CRISPR-Cas, will likely reduce
184 phylogenetic signal.
185
186 As an additional test of the influence of phylogenetic effects on our results, we
187 assessed the impact of including archaeal abundance in our analyses. Archaea have
188 previously been shown to be enriched for CRISPR-Cas systems [1]; therefore,
189 inclusion of archaeal abundance in our model should control for this effect. When we
190 repeated our analysis of the correlation between CRISPR-Cas abundance and viral
191 abundance, this time including the abundance of archaea in each sample as a
192 covariate, we found no qualitative difference in result. Taken with the community
193 composition analysis, these results suggests that the influence of phylogeny on our
194 results is relatively small compared to the effect of viral abundance on the
195 prevalence of CRISPR-Cas immune systems within a microbiome.
196
197

198 ***CRISPR-Cas and viral abundance correlate across diverse environments***
199 To explore to what extent the observed variation in CRISPR-Cas abundance within
200 and between environment types is driven by variation in viral abundance, we
201 grouped the samples by EMPO classification and quantified viral abundance for
202 each environment type. Similarly, to the distributions of CRISPR-Cas abundance, we
203 found substantial variation in viral abundance across environment types (Fig. S2).
204 The higher-level classifications, EMPO level 1 and 2, explained 30% and 31% of the
205 variation observed respectively, and the finer scale EMPO level 3 explained 34% of
206 this variation in viral abundance (GLM, $F_{1,285} = 13.14$, $p < 0.0001$, $R^2 = 0.34$, Fig.
207 S2C). The relatively minor difference between classification levels suggests that the
208 primary predictive power comes from EMPO level 1, with host-associated samples
209 having a greater density of viruses than free-living samples. Overall, we found that
210 the type of environment significantly predicts the abundance of viruses present, but
211 that fine scale classification adds little predictive power relative to high-level
212 classification.
213
214 Although we found a significant correlation between viral abundance and CRISPR-
215 Cas abundance, it remained unclear whether this relationship was consistent across
216 environments. We therefore assessed whether the strength of this relationship was
217 constant among each of our EMPO classification levels, which we modelled as an
218 interaction in a multiple regression analysis. Strikingly, we found significant
219 interaction effects at all EMPO levels, suggesting that the nature of the relationship
220 between viral abundance and CRISPR-Cas abundance is, at least partly, dependent
221 on additional environmental conditions (Table 1, Fig. 3). This was further validated
222 by post-hoc testing of the correlation between CRISPR-Cas abundance and viral
223 abundance at each individual environment type (Table S3). In this case we found a
224 consistent positive relationship at EMPO levels 1 and 2, but more varied results at
225 level 3 (Fig. 3), suggesting additional ecological factors may be playing a role in
226 some environments. For example, when taking all EMPO level 3 classifications with
227 more than 10 observations per group, non-saline sediments show a strong positive
228 correlation between CRISPR-Cas abundance and viral abundance (adjusted p-value
229 < 0.001, Pearson correlation = 0.71, n = 15). In contrast, non-saline water
230 environmental samples show no significant correlation between CRISPR-Cas
231 abundance and viral abundance (adjusted p-value = 1, Pearson correlation = -0.18,

n = 34). All correlations can be found in Table S4. Taken together, these results indicate that viral abundance typically correlates positively with CRISPR-Cas abundance, but that the strength of this relationship is dependent on the particular environment.

Table 1. Interaction effects between virus abundance and CRISPR across environments. Linear models used to test the relationship between CRISPR abundance (DR count) and viral abundance at each EMPO classification level.

Resid. Df	Resid. Dev	df	Deviance	F-value	P-value	AIC	R^2	Model formula
294	15.345	-1	-0.288	5.595	0.019	-32.758	0.224	glm(log10(DR_count) ~ log10(viral_abund) * EMPO_level1
293	15.308	-2	-0.789	7.908	<0.001	-39.572	0.252	glm(log10(DR_count) ~ log10(viral_abund) * EMPO_level2
284	12.074	-9	-1.086	3.02	0.002	-90.349	0.434	glm(log10(DR_count) ~ log10(viral_abund) * EMPO_level3

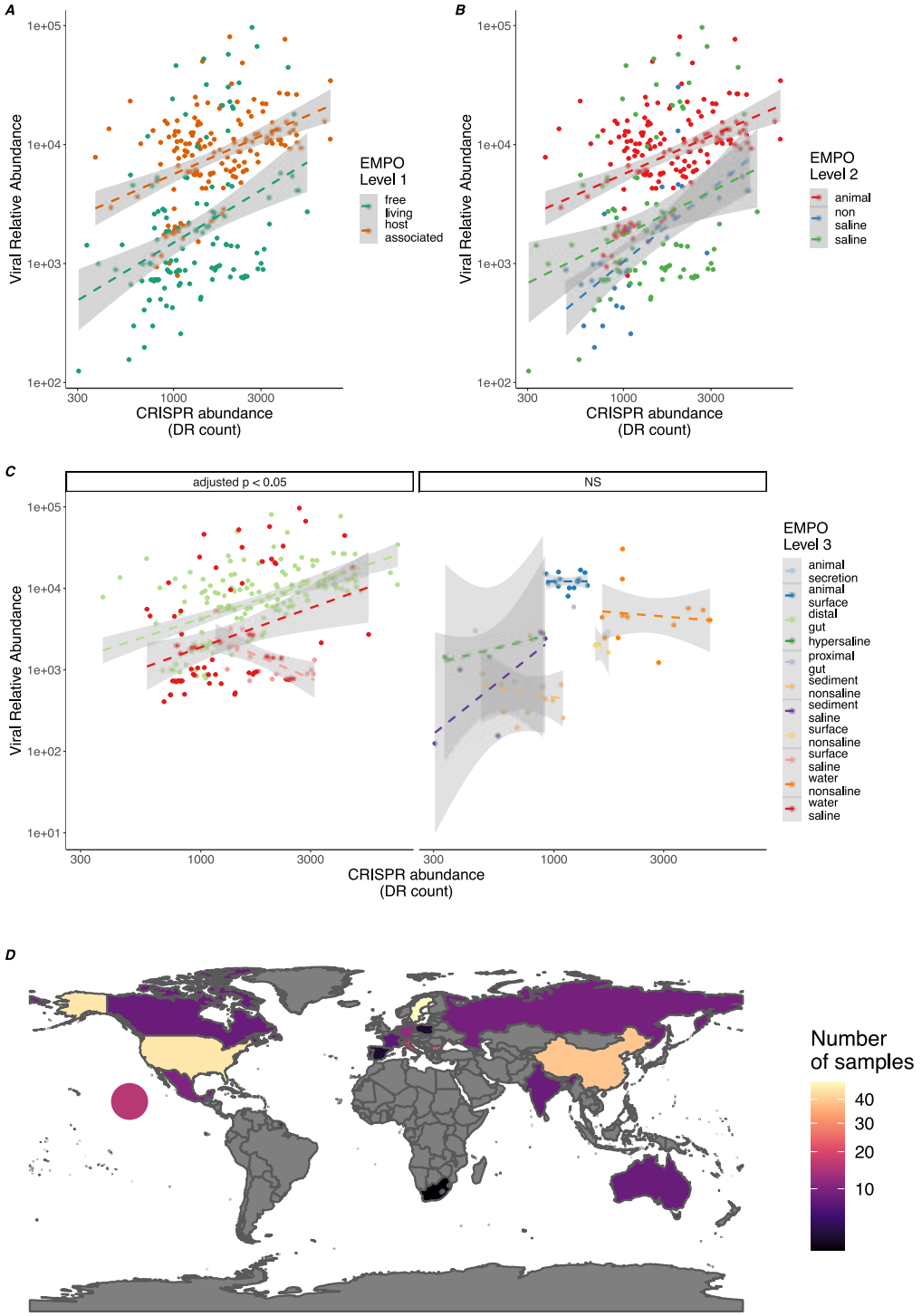

Figure 3. CRISPR abundance positively correlates with viral abundance across environments. Correlations between relative viral abundance and the read count (per million) of metagenomic reads that mapped to CRISPR array repeats per environment type. Environments are categorised according to the Earth Microbiome Project Ontology at level 1 (A) or 2 (B). Samples grouped at EMPO level 3 (C) are divided into significant correlations or non-significant correlations (NS). Dashed lines represent linear model fits and shaded areas represent 95% confidence intervals. (D) The number of samples collected in each country with the circle representing samples collected in the Pacific Ocean.

253 ***Virus diversity negatively correlates with CRISPR-Cas abundance***

254 Both theory and *in vitro* experiments predict that low viral genetic diversity is also an
255 important determinant of the benefits of a CRISPR-Cas immunity [7–9, 11]. This
256 theory suggests that excess viral sequence diversity prevents the acquisition of
257 sufficient spacer diversity to protect against the many different viruses. To test this
258 prediction, we quantified viral diversity for each environment type and examined if
259 this correlated with CRISPR-Cas abundance. However, this analysis may be
260 confounded by correlations between viral diversity and viral abundance. Indeed, in
261 our dataset viral diversity was strongly correlated with viral abundance (GLM, $F_{1,295}$ =
262 208.6, $p < 0.0001$, $R^2 = 0.41$, Fig. S4). We therefore normalized the viral diversity
263 scores by viral abundance for each sample. We then tested the correlation between
264 CRISPR-Cas abundance and normalized viral diversity. In agreement with theory,
265 we found a negative correlation between CRISPR-Cas abundance and normalized
266 viral diversity for all viral diversity metrics used (Fig. 4, Table 2). The metrics used
267 spanned multiple levels, with richness, evenness and Shannon's index describing
268 inter-population diversity. By contrast, Nei's diversity metric describes the intra-
269 population genetic variation. Together these results suggest that CRISPR-Cas is
270 most effective when viral diversity is low, which supports that CRISPR-Cas immunity
271 relies on sequence identity between spacer sequences and the viral protospacer
272 sequence and array sizes are finite.

273

274 **Table 2. Associations between normalized viral diversity metrics and CRISPR abundance.**
275 Results from F-tests using linear models with Bonferroni adjusted p-values for the number of metrics
276 tested (n = 4).

metric	F_value	P_value	Adjusted_p_value
shannon	82.954	<0.001	<0.001
richness	51.899	<0.001	<0.001
evenness	82.091	<0.001	<0.001
nei	65.859	<0.001	<0.001

277

278

279

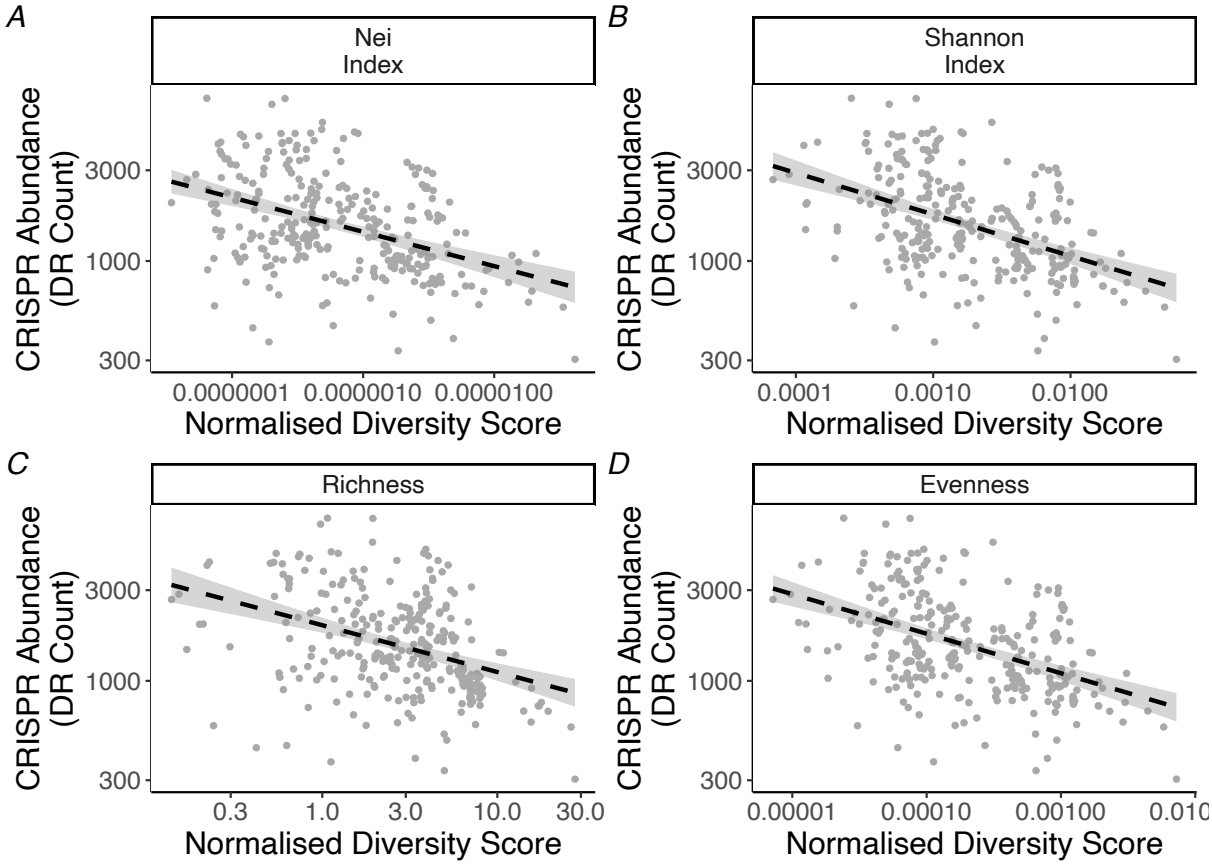

Figure 4. CRISPR abundance negatively correlates with normalised viral diversity metrics. Correlations between viral diversity (normalized by viral load per sample) and CRISPR abundance (reads per million that map to CRISPR arrays). Panels represent Nei's diversity index (A), Shannon's index (B), contig richness (C), contig evenness (D). Panel A represents intra-contig viral diversity while panels B, C and D represent inter-contig viral diversity.

Discussion

Despite recent studies suggesting that CRISPR-Cas abundance varies across natural environments, such as soil [15] and the human microbiome [16], the ecological factors that drive variation in CRISPR-Cas prevalence across natural microbial communities remained unclear [12]. Furthermore, the extent of this variation across a much wider range of environments remained unexplored. We addressed this gap by using metagenomic data to quantify CRISPR array abundance within each metagenome and linked these data to the associated viral community present. We identified two key factors that predict CRISPR-Cas abundance: viral abundance and viral diversity. These factors are likely of primary importance as the observed correlations are consistent across a broad range of environments. Taken together, our results show that high viral abundance and low diversity are major drivers of the selection and maintenance CRISPR-Cas systems in nature.

There are likely factors in addition to viral abundance and diversity that contribute to CRISPR-Cas abundance in the environment because the correlations had relatively low R^2 values (20% for abundance and 22% for normalized diversity). For example, many alternative phage defence systems have been described and, much like CRISPR-Cas, show scattered distributions even in closely related bacterial strains [17]. The interplay and redundancy between different phage defence systems is poorly characterised and may also contribute to CRISPR-Cas distributions in different environments. Understanding the environmental parameters that different defences will be crucial future research. For example, we see greater CRISPR-Cas abundance in host-associated samples over free-living samples, but it is unknown if alternative defence mechanisms are favoured in these free-living samples, or if there are fewer defences overall.

Regarding CRISPR-Cas, multiple environmental parameters have been predicted to interact negatively with these systems. For example, aerobicity showed a negative association with CRISPR-Cas prevalence during a modelling analysis of bacterial traits [13], possibly due to an incompatibility between the requirement for non-homologous end join repair (NHEJ) in aerobic respiration and type II CRISPR-Cas sytems [18]. More generally, intracellular defences may be favoured over surface

333 receptor modifications under certain environmental conditions, as these have been
334 shown to be subject to trade-offs with both biotic and abiotic factors [19–21]. In
335 addition, recent work has demonstrated that regulation of phage defences, including
336 CRISPR-Cas, is mediated by environmental conditions [22]. We also cannot exclude
337 the role of plasmids in our analyses, as a recent longitudinal study found plasmids
338 were targeted by CRISPR-Cas systems at 5-times the rate of phages [23]. Overall,
339 our results demonstrate that phage-mediated selection is a major driver of CRISPR-
340 Cas prevalence, but additional biotic and abiotic complexity likely shape the strength
341 of this relationship.
342
343 Previous theoretical models predicted that CRISPR-Cas will be less favourable in
344 dense and diverse viral communities [8, 9]. Above a threshold of phage genetic
345 diversity CRISPR-Cas becomes ineffective and is lost due an associated fitness cost
346 and this threshold is reached more often in large viral populations [8]. While these
347 predictions are intuitive, our results suggest that while low viral diversity does indeed
348 favour CRISPR-Cas, low viral density does not. It is possible that viral abundance
349 rarely reaches levels in nature that are sufficient to preclude an effective CRISPR-
350 Cas response, even if such densities are readily achievable in laboratory
351 experiments [10, 12]. Future work may reveal the ecological differences between
352 CRISPR-Cas types, as different types are likely to coevolve with viruses in
353 fundamentally different ways [24].
354
355 Genomic evidence demonstrate that CRISPR-Cas systems are frequently acquired
356 and lost [25, 26] and empirical studies that show that they can be mobilized through
357 HGT [27, 28]. Notably, in a previous longitudinal study, CRISPR-Cas abundance
358 increased through time even in phyla decreasing in abundance under soil warming
359 conditions [15], again suggesting high mobility and positive selection for CRISPR-
360 Cas immunity. Consistent with high rates of HGT of CRISPR-Cas, our results
361 demonstrate that while phylogeny can influence the CRISPR-Cas repertoire, it is not
362 the primary driver of selection in nature.
363
364 In summary, by quantifying the role of the viral community in shaping CRISPR-Cas
365 abundance in complex, diverse natural communities we found that high viral
366 abundance, but low diversity, drives the selection and maintenance of CRISPR-Cas

367 across a range of environments. Future work that embraces both the abiotic and
368 biotic complexity of natural systems is required to further understand the prevalence
369 of CRISPR-Cas.
370
371 **Methods**
372 ***Computational pipeline***
373 An overview of the computational pipeline is provided in Figure S1.
374
375 ***Collection of samples and assembly***
376 Paired-end metagenomic libraries (sequenced with Illumina platform) were
377 downloaded from the NCBI SRA database (Table S1). Libraries were processed with
378 BBMap suite of tools for error correction [12] and for each metagenomic library a
379 representative FASTA file was created by combining both the merged and unmerged
380 reads. A total of 332 libraries (each library containing at least 1 million reads with a
381 minimum length of 100 nucleotides (nt) and insert size >=150) were selected to
382 represent a wide range of biome diversity (table S1). Libraries were assembled using
383 MegaHit (version 1.1.3) [13] with default parameters and contigs with minimum
384 length 200nt were retained. Contigs were classified as archaea, bacteria or virus
385 using a purpose-built classification tool: MIUMS (Microbial Identification Using
386 Marker Sequence, https://github.com/ambarishbiswas/miums_v1.0). MIUMS is
387 designed to classify contigs based on a reference database containing protein
388 sequence fragments highly specific to bacteria, archaea, viruses. Full details of
389 MIUMS reference database construction and prediction process are given in the
390 supplementary information. Each metagenome was then subsampled to 1 million
391 randomly selected reads with a minimum length of 100 nt.
392
393 ***Generation of archaeal and bacterial abundance tables***
394 Subsampled reads were screened using metaxa2 [14] (GSU parameters: -g ssu -f f,
395 LSU parameters: -g lsu -f f) to generate a table of bacterial and archaeal
396 abundances. Both the LSU and SSU based methods were used. A reference
397 sequence database was made from contigs classified as viral by MIUMS.
398 Subsampled reads were then mapped to the assembled contigs using Magic-BLAST
399 [15] (parameters: -no_unaligned -no_query_id_trim -perc_identity 95 -outfmt tabular).
400 Reads with a minimum of 95% sequence identity and coverage were used.

401 ***CRISPR array identification***

402 Accurately identifying CRISPR arrays in metagenomic data is challenging for a
403 number of reasons. Firstly, a large proportion of the direct repeats (DRs) identified
404 from metagenomic contigs often show little sequence similarity to the CRISPR
405 repeats found in published genomes and lack an isolated representative [2].
406 Secondly, CRISPR arrays found in metagenomic reads are generally short (i.e. < 3
407 DRs) and often missing one or both flanking regions. To overcome these issues we
408 combined information on existing, published genomes and their CRISPR arrays as
409 well *de novo* extraction of putative CRISPR arrays from our assembled contigs (Fig.
410 S1). A database of metagenomic CRISPR arrays was first constructed by processing
411 all assembled contigs with CRISPRDetect version 3 (CRISPRDetect3,
412 https://github.com/ambarishbiswas/CRISPRDetect_3.0). CRISPRDetect version 3
413 was also modified to allow prediction of shorter CRISPRs (e.g. partial/broken
414 CRISPRs with as little as 1.5 repeats). A higher CRISPR likelihood score cut-off of
415 4.5 was used instead of the default score cut-off of 3 to reduce potential non-
416 CRISPR arrays. CRISPRDetect [16] uses several CRISPR elements (e.g. repeats,
417 spacers, cas genes, AT composition of flanking regions etc.) from published
418 genomes to identify and separate true CRISPRs from other genomic repeats. In this
419 study, a modified version of the CRISPRDetect tool was used, which uses a
420 reference repeat database created using the cluster representative DRs from the
421 metagenomic contigs as well as DRs found in published genomes. Predicted
422 CRISPR arrays were checked to ensure that the total array degeneracy (i.e. number
423 of insertion, deletion, mutation or presence of Ns in the array) was less than the total
424 number of DRs in the array, which resulted in 51395 CRISPR arrays. Direct repeat
425 sequences (23 to 60 nt) were extracted and clustered with cd-hit-est (parameters: -n
426 3 -c 0.90 -aL 0.90 -aS 0.90) [17], which resulted in 33745 repeat clusters. A vast
427 majority of these clusters (i.e. 22808) consisted of a single DR. This low level of
428 redundancy was important to ensure the successful subsequent mapping of reads to
429 DRs.

430

431 Subsampled reads were then screened against this database using
432 metaCRISPRDetect (https://github.com/ambarishbiswas/metaCRISPRDetect_1.0),
433 which supports rapid identification of CRISPR arrays in short reads using user-
434 provided reference repeat database as an extension of CRISPRDetect [16]. Arrays

435 with a likelihood score > 3 were added to the existing CRISPR reference database.
436 Subsampled reads were then mapped to the reference database using blastn [18]
437 [parameters: -task blastn-short with default parameters]. Abundance tables were
438 generated for all spacers and direct repeat sequences by tallying the number of
439 reads that mapped to a given DR with 100% sequence identity and coverage.
440
441 ***Identifying potential false positive CRISPRs***
442 CRISPRs predicted from metagenomes are generally short, often incomplete and
443 missing flanking regions which makes it hard to distinguish true CRISPRs from other
444 genomic repeats. To measure how many of our identified arrays occurred in known
445 prokaryotic genomes we compared the metagenomic CRISPR repeats against
446 CRISPRs found in RefSeq and GenBank prokaryotic sequences (sequences
447 published before September 9, 2019) using NCBI blast (parameters: -task blastn -
448 word_size 11 -dust no -culling_limit 1 -num_alignments 1) [19]. Metagenomic DRs
449 with >=90% identity and >=90% sequence coverage against RefSeq or GenBank
450 DRs were considered as a positive match. Out of the 7562 repeat clusters 1649
451 were found in CRISPRs predicted from RefSeq or GenBank prokaryotic sequences.
452 Similarly, the metagenomic repeats were screened against an *in silico* generated set
453 of eukaryotic reads from 6 eukaryotic reference genomes (Table S2). Ten thousand
454 250bp paired reads were generated from each reference genome using WGSIM
455 (https://github.com/lh3/wgsim). Eukaryotic reads were subsampled to an equal depth
456 to remove differences due to genome size. Out of the 7562 DR clusters a total of 168
457 repeat clusters were found in the eukaryotic reads suggesting a high level of
458 eukaryotic sequence contamination may increase the false positive rate of our
459 analysis. We therefore removed samples where > 10% of reads were classified as of
460 eukaryotic origin.
461
462 ***Virome analysis***
463 To assess the diversity of viruses in the different environments, we analysed all
464 MIUMS classified contigs from the 332 metagenomes. Across all datasets, we
465 identified 2583 archaeal prophages, 375179 bacterial prophages, 1218279
466 bacteriophages, and 174792 archaeal viruses. Per metagenome, the sub-sampled
467 reads used for the CRISPR quantification analysis were mapped to the total set of all
468 viral contigs with bwa mem [20]. To quantify the genetic diversity of the viral

469 community, we calculated the richness as the total number of detected viral contigs,
470 plus the evenness and Shannon's diversity index based on relative abundances
471 calculated from the mean depth of coverage of all detected viral contigs. The intra-
472 population diversity (micro-diversity) was calculated as the mean heterozygosity of
473 viruses in the community by averaging Nei's per-nucleotide diversity index across all
474 detected contigs [21].
475

476 $$Nei = \frac{1}{L * N} \sum_{i=1}^{L} (1 - \sum_{j=1}^{n} p_j^2)$$

477
478 where p_j is the frequency of allele *j* at the position *i* of a contig of the length L, N is
479 the number of viruses in a dataset. Single nucleotide variability was assessed with
480 VarScan software [22].
481
482 Viral abundance was calculated by first collecting the average depth values for all
483 viral contigs in each sample using the 'jgi_summarize_bam_contig_depths' script
484 from the Metabat package [23]. These depth scores were then summed per sample
485 to give an approximation of overall viral abundance relative to bacterial abundance.
486
487 ***Statistical analysis***
488 For each sample, the number of reads that mapped to a direct repeat were counted
489 to give a measure of CRISPR array abundance per sample. Earth Microbiome
490 Project Ontology levels were assigned using the framework previously described
491 [24](Fig 1D) based on the associated metadata from the NCBI short read archive
492 (SRA). In the case of bioreactor samples, a literature search was conducted to
493 identify the original material described in the associated study (see Table S1).
494
495 General linear models (GLM) were constructed for each of the reported correlations.
496 In each case log10 transformations were applied to conform to model assumptions.
497 Checks of model residuals were performed to assess model fit. Significance was
498 determined using F-tests between null models and those containing the variable or
499 interaction of interest.
500

501 ***Microbial community assessment***

502 CRISPR is more common in archaea. Therefore, in order to minimise any
503 phylogenetic effects deriving from high archaeal abundances in samples we
504 estimated the number of archaeal reads in the subsampled reads using metaxa2 [14]
505 and converted this to relative abundance per sample. We then included this value as
506 a fixed effect in additional GLMs to check the influence of archaeal abundance on
507 our results. For additional phylogenetic assessments, reads classified as non-
508 prokaryotic were removed and relative abundances were generated using the output
509 from metaxa2 in order to assess effects of community composition. Permutational
510 ANOVAs were performed on species abundance matrices using Bray-Curtis
511 dissimilarity and CRISPR abundance as explanatory variable with 9999
512 permutations, using the function 'adonis' from 'vegan' package [25]. Visualisation of
513 clustering analyses, at the class level, was performed using non-metric
514 multidimensional scaling (NMDS) with Bray-Curtis dissimilarity through the
515 'metaMDS' function in 'vegan' [25]. Smooth surfaces were fit to these points via a
516 generalized additive model (GAM), using either CRISPR abundance as the
517 explanatory term, with the 'ordisurf' function in 'vegan'[25].
518

519 **Acknowledgments**

520 This work was funded by a grant from the European Research Council under the
521 European Union's Horizon 2020 research and innovation programme (ERC-STG-
522 2016-714478 to E.R.W.) E.R.W. was further supported by a NERC Independent
523 Research Fellowship (NE/M018350/1). S.M. received funding from the European
524 Union's Horizon 2020 research and innovation programme under the Marie
525 Skłodowska-Curie grant agreement No. 842656. B.E.D was supported by the
526 Netherlands Organization for Scientific Research (NWO) Vidi grant 864.14.004 and
527 European Research Council (ERC) Consolidator grant 865694: DiversiPHI. P.C.F.
528 was supported by the Bio-protection Research Centre (Tertiary Education
529 Commission (TEC), New Zealand.
530
531
532
533
534

535 **Author contributions**

536 **Conceptualization**, B.E.D., E.W., P.F. and S.E.M; **Methodology**, A.B., B.E.D.,
537 E.W., K.A., P.F., S.E.M and S.M; **Software**, A.B., B.E.D. and K.A.; **Formal analysis**,
538 A.B., B.E.D., K.A. and S.M.; **Investigation**, A.B., B.E.D., K.A., and S.M.; **Data**
539 **Curation**, A.B., B.E.D., K.A. and S.M.; **Writing – Original draft**, E.W., P.F. and
540 S.M.; **Writing – Review & Editing**, A.B., B.E.D., E.W., K.A., P.F., S.E.M, and S.M.;
541 **Visualization**, S.M.; **Supervision**, B.E.D., E.W., P.F. and S.E.M.; **Project**
542 **Administration**, B.E.D., E.W., S.E.M. and P.F.; **Funding acquisition**, B.E.D., E.W.,
543 S.E.M., S.M. and P.F.

544

545 **References**

546 1. Makarova, K.S., Wolf, Y.I., Iranzo, J., Shmakov, S.A., Alkhnbashi, O.S.,
547 Brouns, S.J., Charpentier, E., Cheng, D., Haft, D.H., Horvath, P. and Moineau, S.,
548 2020. Evolutionary classification of CRISPR–Cas systems: a burst of class 2 and
549 derived variants. *Nature Reviews Microbiology*, *18*(2), pp.67-83

550

551 2. Burstein, D., Sun, C.L., Brown, C.T., Sharon, I., Anantharaman, K., Probst,
552 A.J., Thomas, B.C. and Banfield, J.F., 2016. Major bacterial lineages are essentially
553 devoid of CRISPR-Cas viral defence systems. *Nature communications*, *7*(1), pp.1-8.

554

555 3. Pourcel, C., Touchon, M., Villeriot, N., Vernadet, J.P., Couvin, D., Toffano-
556 Nioche, C. and Vergnaud, G., 2020. CRISPRCasdb a successor of CRISPRdb
557 containing CRISPR arrays and cas genes from complete genome sequences, and
558 tools to download and query lists of repeats and spacers. *Nucleic acids*
559 *research*, *48*(D1), pp.D535-D544.

560

561 4. Mojica, F.J. and Garrett, R.A., 2013. Discovery and seminal developments in
562 the CRISPR field. In *CRISPR-Cas Systems* (pp. 1-31). Springer, Berlin, Heidelber

563

564 5. Makarova, K.S., Wolf, Y.I. and Koonin, E.V., 2013. Comparative genomics of
565 defense systems in archaea and bacteria. *Nucleic acids research*, *41*(8), pp.4360-
566 4377.

567

6. Hille, F., Richter, H., Wong, S.P., Bratovič, M., Ressel, S. and Charpentier, E., 2018. The biology of CRISPR-Cas: backward and forward. *Cell*, *172*(6), pp.1239-1259.

7. Gurney, J., Pleška, M. and Levin, B.R., 2019. Why put up with immunity when there is resistance: an excursion into the population and evolutionary dynamics of restriction–modification and CRISPR-Cas. *Philosophical Transactions of the Royal Society B*, *374*(1772), p.20180096.

8. Iranzo, J., Lobkovsky, A.E., Wolf, Y.I. and Koonin, E.V., 2013. Evolutionary dynamics of the prokaryotic adaptive immunity system CRISPR-Cas in an explicit ecological context. *Journal of bacteriology*, *195*(17), pp.3834-3844.

9. Weinberger, A.D., Sun, C.L., Pluciński, M.M., Denef, V.J., Thomas, B.C., Horvath, P., Barrangou, R., Gilmore, M.S., Getz, W.M. and Banfield, J.F., 2012. Persisting viral sequences shape microbial CRISPR-based immunity. *PLoS Comput Biol*, *8*(4), p.e1002475.

10. Westra, E.R., van Houte, S., Oyesiku-Blakemore, S., Makin, B., Broniewski, J.M., Best, A., Bondy-Denomy, J., Davidson, A., Boots, M. and Buckling, A., 2015. Parasite exposure drives selective evolution of constitutive versus inducible defense. *Current biology*, *25*(8), pp.1043-1049.

11. Broniewski, J.M., Meaden, S., Paterson, S., Buckling, A. and Westra, E.R., 2020. The effect of phage genetic diversity on bacterial resistance evolution. *The ISME journal*, *14*(3), pp.828-836.

12. Westra, E.R. and Levin, B.R., 2020. It is unclear how important CRISPR-Cas systems are for protecting natural populations of bacteria against infections by mobile genetic elements. *Proceedings of the National Academy of Sciences*, *117*(45), pp.27777-27785.

600 13. Weissman, J.L., Laljani, R.M., Fagan, W.F. and Johnson, P.L., 2019.
601 Visualization and prediction of CRISPR incidence in microbial trait-space to identify
602 drivers of antiviral immune strategy. *The ISME journal*, *13*(10), pp.2589-2602.
603
604 14. Thompson, L.R., Sanders, J.G., McDonald, D., Amir, A., Ladau, J., Locey,
605 K.J., Prill, R.J., Tripathi, A., Gibbons, S.M., Ackermann, G. and Navas-Molina, J.A.,
606 2017. A communal catalogue reveals Earth's multiscale microbial
607 diversity. *Nature*, *551*(7681), pp.457-463.
608
609 15. Wu, R., Chai, B., Cole, J.R., Gunturu, S.K., Guo, X., Tian, R., Gu, J.D., Zhou,
610 J. and Tiedje, J.M., 2020. Targeted assemblies of cas1 suggest CRISPR-Cas's
611 response to soil warming. *The ISME journal*, pp.1-12.
612
613 16. Münch, P.C., Franzosa, E.A., Stecher, B., McHardy, A.C. and Huttenhower,
614 C., 2021. Identification of Natural CRISPR Systems and Targets in the Human
615 Microbiome. *Cell Host & Microbe*, *29*(1), pp.94-106.
616
617 17. Bernheim, A. and Sorek, R., 2020. The pan-immune system of bacteria:
618 antiviral defence as a community resource. *Nature Reviews Microbiology*, *18*(2),
619 pp.113-119.
620
621 18. Bernheim, A., Calvo-Villamañán, A., Basier, C., Cui, L., Rocha, E.P.,
622 Touchon, M. and Bikard, D., 2017. Inhibition of NHEJ repair by type II-A CRISPR-
623 Cas systems in bacteria. *Nature communications*, *8*(1), pp.1-9.
624
625 19. Hernandez, C.A. and Koskella, B., 2019. Phage resistance evolution in vitro is
626 not reflective of in vivo outcome in a plant-bacteria-phage system. *Evolution*, *73*(12),
627 pp.2461-2475.
628
629 20. Laanto, E., Bamford, J.K., Laakso, J. and Sundberg, L.R., 2012. Phage-driven
630 loss of virulence in a fish pathogenic bacterium. *PLoS One*, *7*(12), p.e53157.
631

632 21. Alseth, E.O., Pursey, E., Luján, A.M., McLeod, I., Rollie, C. and Westra, E.R.,
633 2019. Bacterial biodiversity drives the evolution of CRISPR-based phage
634 resistance. *Nature*, *574*(7779), pp.549-552.
635
636 22. Smith, L.M., Jackson, S.A., Malone, L.M., Ussher, J.E., Gardner, P.P. and
637 Fineran, P.C., 2021. The Rcs stress response inversely controls surface and
638 CRISPR–Cas adaptive immunity to discriminate plasmids and phages. *Nature*
639 *Microbiology*, *6*(2), pp.162-172.
640
641 23. Arbas, S.M., Narayanasamy, S., Herold, M., Lebrun, L.A., Hoopmann, M.R.,
642 Li, S., Lam, T.J., Kunath, B.J., Hicks, N.D., Liu, C.M. and Price, L.B., 2021. Roles of
643 bacteriophages, plasmids and CRISPR immunity in microbial community dynamics
644 revealed using time-series integrated meta-omics. *Nature microbiology*, *6*(1), pp.123-
645 135.
646
647 24. Watson, B.N., Steens, J.A., Staals, R.H., Westra, E.R. and van Houte, S.,
648 2021. Coevolution between bacterial CRISPR-Cas systems and their
649 bacteriophages. *Cell Host & Microbe*, *29*(5), pp.715-725.
650
651 25. Puigbò, P., Makarova, K.S., Kristensen, D.M., Wolf, Y.I. and Koonin, E.V.,
652 2017. Reconstruction of the evolution of microbial defense systems. *BMC*
653 *evolutionary biology*, *17*(1), pp.1-13.
654
655 26. van Belkum, A., Soriaga, L.B., LaFave, M.C., Akella, S., Veyrieras, J.B.,
656 Barbu, E.M., Shortridge, D., Blanc, B., Hannum, G., Zambardi, G. and Miller, K.,
657 2015. Phylogenetic distribution of CRISPR-Cas systems in antibiotic-resistant
658 Pseudomonas aeruginosa. *MBio*, *6*(6), pp.e01796-15.
659
660 27. Watson, B.N., Staals, R.H. and Fineran, P.C., 2018. CRISPR-Cas-mediated
661 phage resistance enhances horizontal gene transfer by transduction. *MBio*, *9*(1),
662 pp.e02406-17.
663

664 28. Varble, A., Meaden, S., Barrangou, R., Westra, E.R. and Marraffini, L.A.,
665 2019. Recombination between phages and CRISPR− cas loci facilitates horizontal
666 gene transfer in staphylococci. *Nature microbiology*, *4*(6), pp.956-963.
667
668 29. Bushnell, B., Rood, J. and Singer, E., 2017. BBMerge–Accurate paired
669 shotgun read merging via overlap. *PloS one*, *12*(10), p.e0185056.
670
671 30. Li, D., Liu, C.M., Luo, R., Sadakane, K. and Lam, T.W., 2015. MEGAHIT: an
672 ultra-fast single-node solution for large and complex metagenomics assembly via
673 succinct de Bruijn graph. *Bioinformatics*, *31*(10), pp.1674-1676.
674
675 31. Bengtsson-Palme, J., Hartmann, M., Eriksson, K.M., Pal, C., Thorell, K.,
676 Larsson, D.G.J. and Nilsson, R.H., 2015. METAXA2: improved identification and
677 taxonomic classification of small and large subunit rRNA in metagenomic
678 data. *Molecular ecology resources*, *15*(6), pp.1403-1414.
679
680 32. Boratyn, G.M., Thierry-Mieg, J., Thierry-Mieg, D., Busby, B. and Madden,
681 T.L., 2019. Magic-BLAST, an accurate RNA-seq aligner for long and short
682 reads. *BMC bioinformatics*, *20*(1), pp.1-19.
683
684 33. Biswas, A., Staals, R.H., Morales, S.E., Fineran, P.C. and Brown, C.M., 2016.
685 CRISPRDetect: a flexible algorithm to define CRISPR arrays. *BMC genomics*, *17*(1),
686 pp.1-14.
687
688 34. Li, W. and Godzik, A., 2006. Cd-hit: a fast program for clustering and
689 comparing large sets of protein or nucleotide sequences. *Bioinformatics*, *22*(13),
690 pp.1658-1659.
691
692 35. Chen, Y., Ye, W., Zhang, Y. and Xu, Y., 2015. High speed BLASTN: an
693 accelerated MegaBLAST search tool. *Nucleic acids research*, *43*(16), pp.7762-7768.
694
695 36. Altschul, S.F., Gish, W., Miller, W., Myers, E.W. and Lipman, D.J., 1990.
696 Basic local alignment search tool. *Journal of molecular biology*, *215*(3), pp.403-410.
697

37. Li, H. and Durbin, R., 2009. Fast and accurate short read alignment with Burrows–Wheeler transform. *bioinformatics*, *25*(14), pp.1754-1760.

38. Nei, M., 1978. Estimation of average heterozygosity and genetic distance from a small number of individuals. *Genetics*, *89*(3), pp.583-590.

39. Koboldt, D.C., Chen, K., Wylie, T., Larson, D.E., McLellan, M.D., Mardis, E.R., Weinstock, G.M., Wilson, R.K. and Ding, L., 2009. VarScan: variant detection in massively parallel sequencing of individual and pooled samples. *Bioinformatics*, *25*(17), pp.2283-2285.

40. Kang, D.D., Froula, J., Egan, R. and Wang, Z., 2015. MetaBAT, an efficient tool for accurately reconstructing single genomes from complex microbial communities. *PeerJ*, *3*, p.e1165.

41. Oksanen, J., Blanchet, F.G., Kindt, R., Legendre, P., Minchin, P.R., O'hara, R.B., Simpson, G.L., Solymos, P., Stevens, M.H.H. and Wagner, H., 2013. Community ecology package. *R package version*, *2*(0)

732 **Supplementary Information**

733 **Supplementary Figures**

734

735

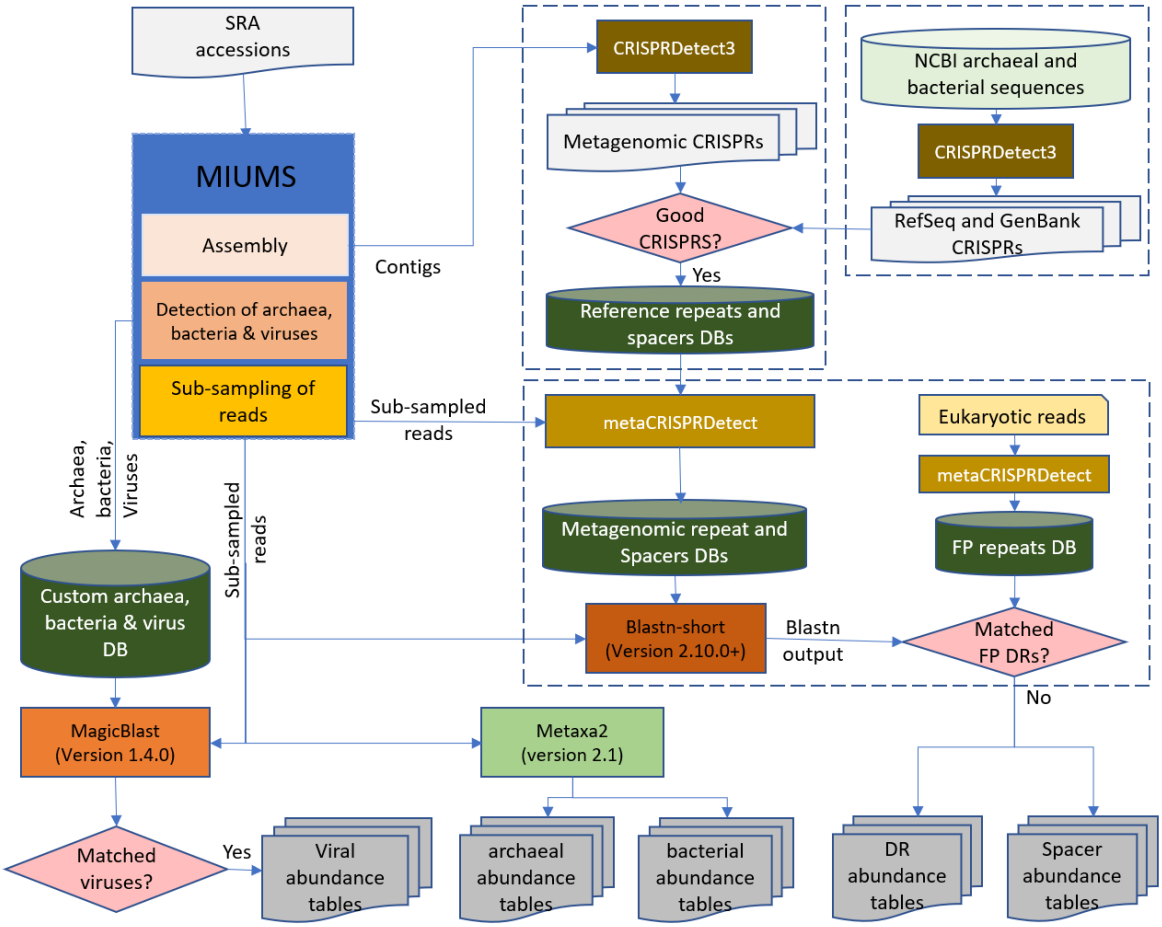

736 **Figure S1. Overview of computational pipeline.** Overview of the computational
737 pipeline used to generate CRISPR abundance tables, microbial and viral community
738 abundance tables. In each stage, only the case (yes/no) where data is retained is
739 presented.

740

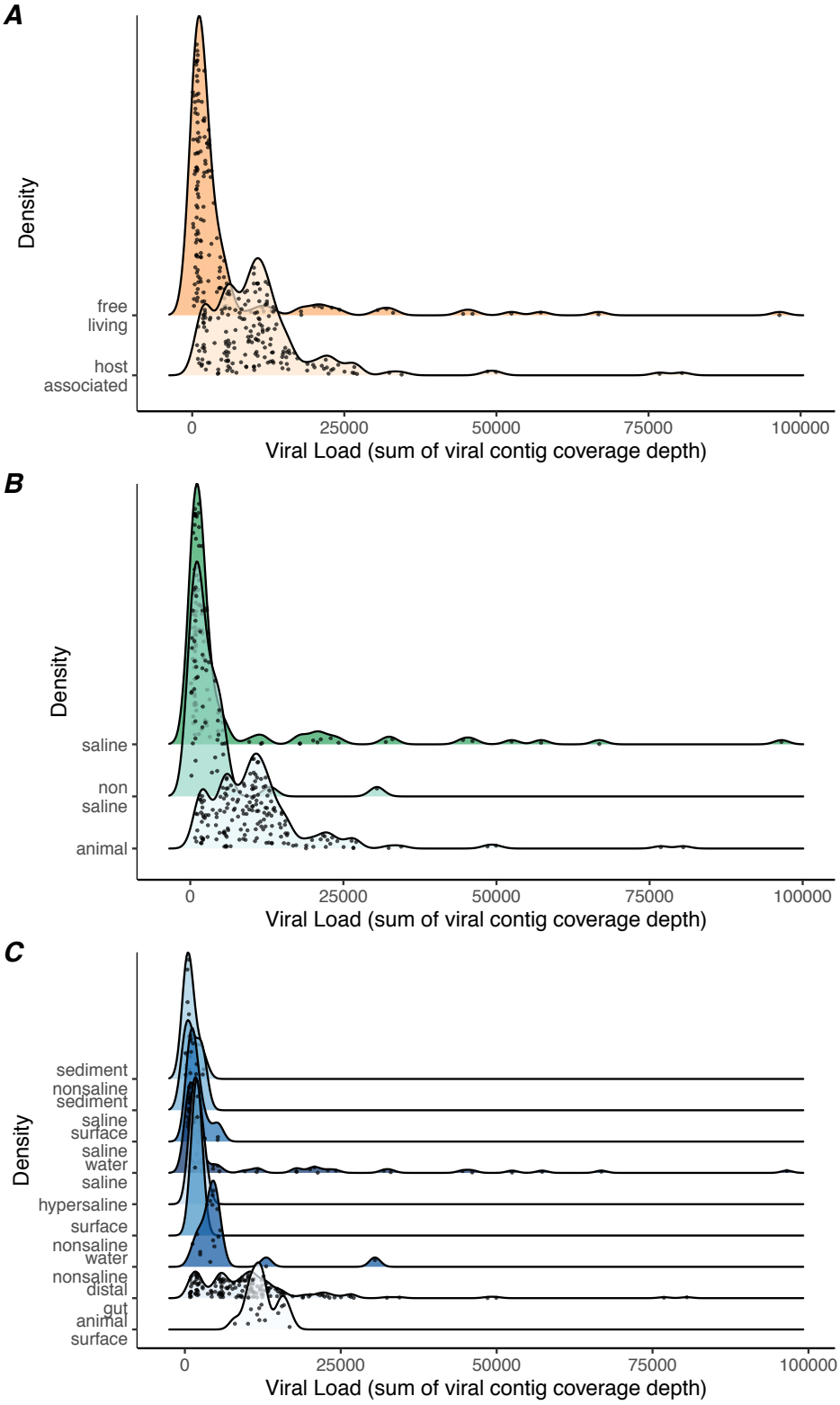

Figure S2. Viral abundance varies by environment. Distributions of viral abundances (sum of viral contig coverage depth per sample) across EMPO level 1 categories (A), level 2 categories (B) and level 3 categories (C). Points represent metagenomic samples.

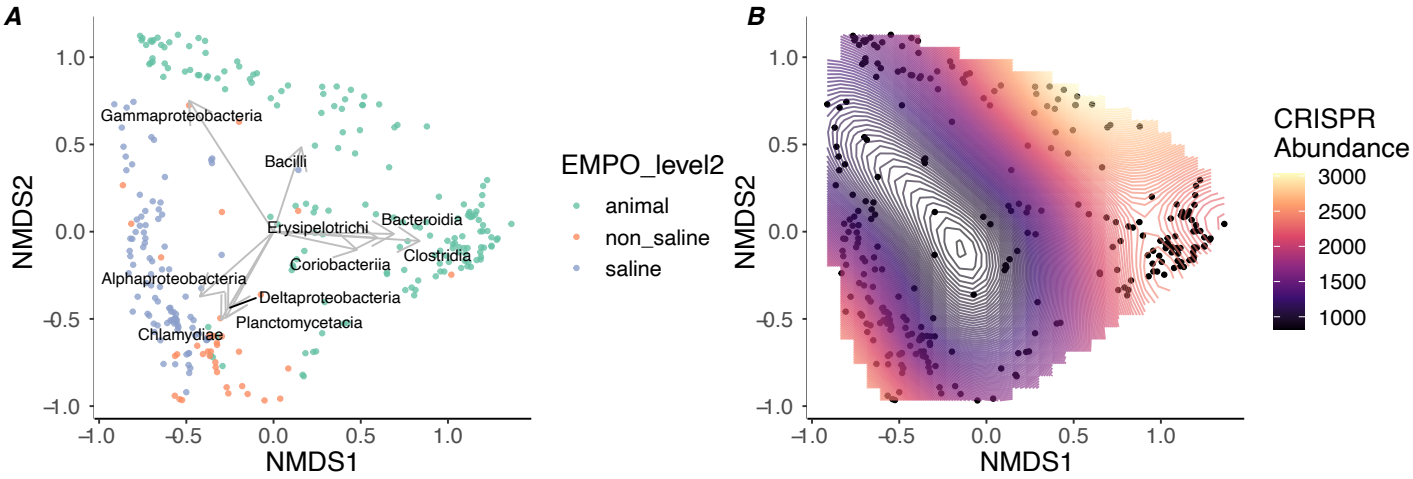

Figure S3. Phylogenetic ordinations of sample community composition. Ordinations of sample community compositions at the Class level. Points represent individual metagenomic samples and are clustered using non-metric multidimensional scaling (NMDS) on Bray-Curtis dissimilarity scores. (*A*) Colors represent the sample classification at EMPO level 2 and arrows represent the top 10 species loadings. (*B*) The same ordination of samples with CRISPR abundance used in a generalized additive model (GAM) to fit a surface predicting CRISPR abundance.

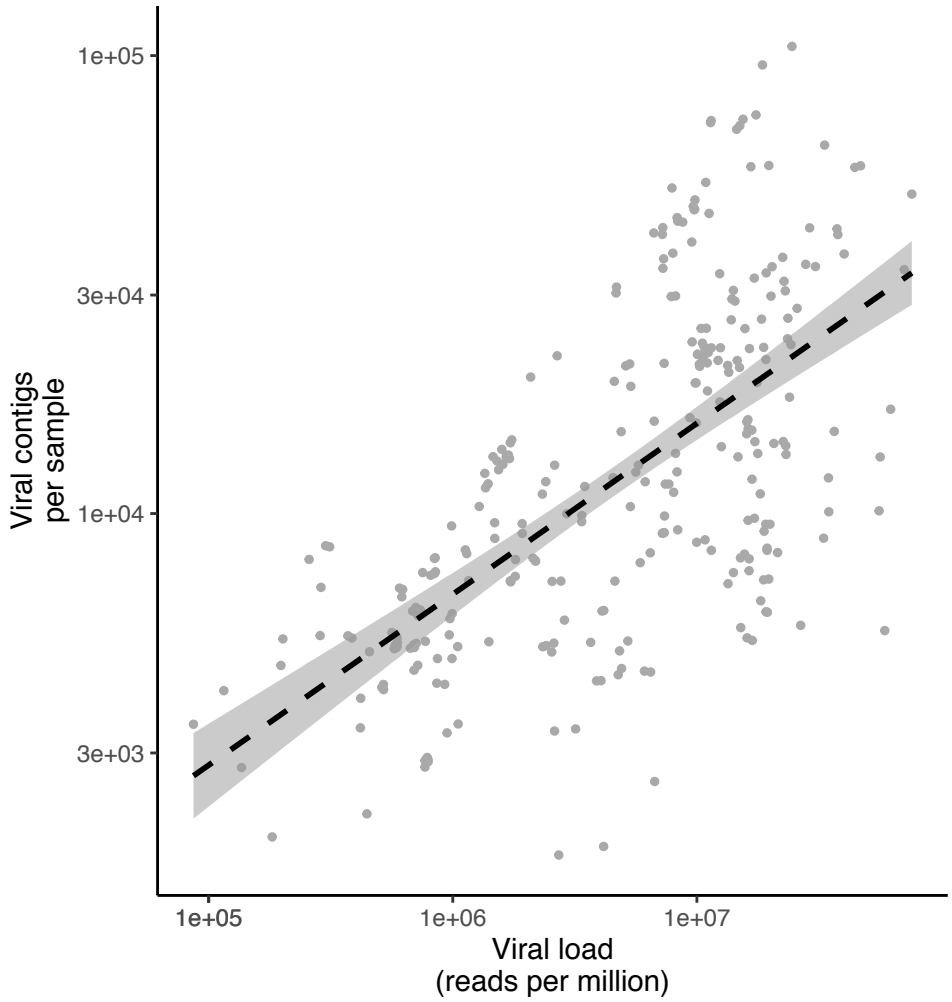

Figure S4. Viral abundance correlates with viral diversity. Correlation between the number of viral contigs per sample and viral abundance (sum of viral contig coverage depth per sample). Line represents linear model fit, shaded areas denote 95% confidence intervals and $R^2 = 0.51$.

775 **Supplementary Tables**

776

777 **Table S1. Biome and accession numbers of each metagenome sample**

778 *table_S1_accesions_meta.csv*

779

780 **Table S2. Eukaryotic genome list used for testing false positive rate.**

781

Species	Genbank accession
Triticum aestivum	GCA_900519105.1
Drosophila melanogaster	GCA_000001215.4
Arabidopsis thaliana	GCA_000001735.1
Physcomitrella patens	GCA_000002425.2
Caenorhabdtitis elegans	GCA_000002985.3
Heliconius melpomene	GCA_000313835.1

782

783

784

785

786

787

788

789

790

791

792

793

794

795

796

797

798

799

Table S3. Post-hoc testing of correlations between CRISPR abundance and viral abundance at each environmental classification. Linear regression of CRISPR abundance with viral abundance for each environmental classification. P-values were adjusted using Benjamini-Hochberg correction. NA results are shown for categories with < 3 observations.

EMPO category	Estimate	Std. Error	t-value	P-value	EMPO level	adjusted-p-value	significance
free_living	0.167	0.034	4.871	<0.001	1	<0.001	***
host_associated	0.305	0.047	6.489	<0.001	1	<0.001	***
animal	0.305	0.047	6.489	<0.001	2	<0.001	***
non_saline	0.392	0.068	5.803	<0.001	2	<0.001	***
saline	0.118	0.039	3.061	0.003	2	0.008	**
animal_secretion	2.66	NA	NA	NaN	3	NaN	NA
animal_surface	0	0.183	0.001	0.999	3	1	
distal_gut	0.328	0.04	8.124	<0.001	3	<0.001	***
hypersaline	1.142	0.565	2.022	0.292	3	0.414	
proximal_gut	3.086	NA	NA	NaN	3	NaN	NA
sediment_nonsaline	-0.059	0.115	-0.513	0.619	3	0.81	
sediment_saline	0.241	0.127	1.891	0.155	3	0.264	
surface_nonsaline	-0.534	0.162	-3.302	0.187	3	0.289	
surface_saline	-0.338	0.102	-3.31	0.004	3	0.009	**
water_nonsaline	-0.063	0.156	-0.403	0.695	3	0.844	
water_saline	0.114	0.038	2.97	0.004	3	0.01	**

811 **Table S4. Pearson correlations of CRISPR abundance and viral abundance at**
812 **each environmental classification.**
813

environment	EMPO level	estimate	p.value	adjusted.p.value
host associated	1	0.318669937	1.62941E-05	0.000179235
free living	1	0.225345517	0.007648844	0.084137289
animal	2	0.318669937	1.62941E-05	0.000179235
saline	2	0.279115129	0.00588914	0.064780536
non saline	2	0.300602925	0.050152056	0.551672619
distal gut	3	0.355793262	2.37403E-06	2.61143E-05
sediment nonsaline	3	0.705624736	0.003291221	0.036203435
water saline	3	0.319818959	0.006956952	0.07652647
surface saline	3	-0.42738303	0.127443734	1
water nonsaline	3	-0.180788442	0.487439096	1
animal surface	3	0.032966836	0.907150313	1

814
815
816
817
818
819
820
821
822
823
824
825

826 **Table S5. Precision and recall analysis of viral classification tools.**

Classifier	Sequence source	Total sequences	Number classified	Correct	Incorrect	False negatives	Precision	Recall
MIUMS	archaea	15000	10128	9362	766	5638	0.95	0.73
MIUMS	bacteria	15000	12782	12582	200	2418	0.99	0.86
MIUMS	**viruses**	**5000**	**2592**	**2560**	**32**	**2440**	**0.99**	**0.67**
MIUMS	eukaryotes	15000	13	0	13	15000	1	0.5
DeepVirFinder	archaea	15000	NA	NA	NA	NA	NA	NA
DeepVirFinder	bacteria	15000	NA	NA	NA	NA	NA	NA
DeepVirFinder	**viruses**	**5000**	**6555**	**2092**	**4463**	**2908**	**0.53**	**0.63**
DeepVirFinder	eukaryotes	15000	NA	NA	NA	NA	NA	NA
VirSorter2	archaea	15000	NA	NA	NA	NA	NA	NA
VirSorter2	bacteria	15000	NA	NA	NA	NA	NA	NA
VirSorter2	**viruses**	**5000**	**3684**	**2367**	**1317**	**2633**	**0.79**	**0.66**
VirSorter2	eukaryotes	15000	NA	NA	NA	NA	NA	NA

827
828
829
830
831
832
833
834
835
836
837
838
839
840
841
842
843
844
845
846
847

848 **Supplemental Methods**

849

850 **Microbial Identification Using Marker Sequence (MIUMS).**

851 MIUMS (version 1.0) utilizes a reference database of protein sequence fragments
852 that are highly specific to their source organism. The process of constructing
853 database is described below.

854

855 **1. Selection of reference sequences**

856 For the construction of a reference database of marker amino acid sequences, all
857 amino acid sequences from 224 archaeal, 2810 bacterial and 3958 viral (4185)
858 species (published before 1st of March 2017; Refseq release version 79; minimum
859 sequence length of 5000 nucleotides) were selected as the source of the protein
860 sequences for the marker sequence database. These resulted in 155585 archaeal,
861 2219071 bacterial and 229026 viral amino acid sequences. In addition, a eukaryotic
862 protein sequence database was constructed from 16179736 eukaryotic proteins. The
863 taxonomic information of these protein sequences were collected from NCBI
864 taxonomy files (https://ftp.ncbi.nlm.nih.gov/pub/taxonomy/).

865

866 **2. Construction of short protein sequence fragments**

867 The construction of a database of marker protein sequence fragments is a multi-step
868 process, which includes i). removal of sequence domains and ii). removal of all
869 potential inter (super)kingdom homologous sequence regions from the target protein
870 sequences.

871

872 The selected protein sequences from archaea, bacteria and viruses were screened
873 with Pfam-A HMM profiles (version 30.0) [1] and hmmsearch (HMMER version 3.2.1
874 with default parameters and --domtblout) [2]. Using the reported domain regions in
875 the sequences, the protein sequences were split into multiple sequence fragments
876 excluding the domain regions.

877

878 The sequence fragments were then concatenated into a single protein sequence
879 database and performed an all-vs-all sequence similarity search using diamond
880 (version v0.8.38.100; parameters: --evalue 0.001 --sensitive --no-self-hits) [3]. By
881 analysing the diamond output file, longer sequence fragments which contain shorter

882 sequence fragments were identified and further split into multiple sequence
883 fragments followed by construction of a new sequence database. This process of
884 identification of shorter sequence fragments continued in a cyclic manner till there
885 were no new fragments identified.
886
887 **3. Removal of inter superkingdom specific protein fragments**
888 The sequence fragments were then separated into their associated superkingdom
889 and screened against the other superkingdom specific primary protein sequences
890 (including eukaryotic protein sequences) using diamond (parameters: --evalue 0.001
891 --sensitive). Sequence fragments that were found to have inter (super)kingdom
892 matches were identified and removed. This resulted in 610460 archaeal, 8312644
893 bacterial and 677951 viral marker protein fragments.
894
895 **4. Assigning taxa specificity to the protein fragments**
896 The archaeal, bacterial, and viral protein fragments were then screened against their
897 own superkingdom specific primary source proteins using diamond (parameters: --
898 evalue 0.001 --sensitive) and the taxa specificity of each protein fragment to each of
899 the higher taxonomic levels (i.e. phylum, class, order, family, genus and species)
900 was determined using lowest common ancestor (LCA) algorithm from all reported
901 diamond matches.
902
903 **Taxonomic classification of metagenomic sequences**
904 The default MIUMS runs involve three steps; i) assembly of metagenomic reads, ii)
905 prediction of protein sequence in the assembled contigs using metaGeneMark [4], iii)
906 screening the protein sequences against the marker protein fragment database
907 using diamond (parameters: --evalue 0.001 --sensitive). Contigs with
908 metaGeneMark predicted proteins that contains multiple matches to the protein
909 fragments above stringency cutoffs (e.g. overlapping length >=21aa and sequence
910 identity >=40%) are assigned taxonomy based on the matched protein fragment's
911 taxa specificity and LCA algorithm. An output table is generated, which shows a list
912 of classified contigs with associated taxonomy.
913 The raw reads (unless a subsampling of the reads were done) were mapped to the
914 entire assembled contigs using magicblast [5]. The magicblast output file is analysed
915 to identify all reads mapping to the classified contigs with minimum 99% identity and

99% sequence coverage. An output table is generated that shows each of those reads and their associated taxonomy.

Benchmarking of viral classification tools

In order to assess the accuracy of MIUMS for extracting viral contigs, we compared against existing tools using a test dataset of known sequences. The reference database of marker protein fragments that MIUMS V1.0 uses was constructed from sequences published before 1st of March 2017. Since then the number of newly released viral sequences in the NCBI RefSeq database has nearly doubled (5343 genomic DNA/RNA sequences published between 01-Mar-2017 and 01-June-2021; with minimum length 500 nucleotides). To assess the performance of MIUMS against these newly published sequences; we randomly added 5000 of these viral sequences in a test dataset, comprising closed, whole genomes and contig-level assemblies. The test dataset was also supplemented with 15000 archaea, 15000 bacteria and 15000 eukaryotic sequences published during the same time period mentioned above (with minimum length cut-off of 500 nucleotides and maximum length of 25000 nucleotides). We also included eukaryotic sequences (randomly selected from animal, plant, fungi and protists sequences). This test dataset was analysed with MIUMS V1.0, VirSorter2 (version 2.2.2) [6] and DeepVirFinder (version 1.0) [7] with default parameters. Table S5 shows the summary outputs from the 3 tools used and their respective precision and recall scores.

DeepVirFinder reports a score between 0 to 1 for every input sequence, where a higher score (i.e. close to 1) is a strong indicator of a sequence being viral. Against a minimum score cutoff of 0.95, DeepVirFinder correctly predicted 2092 viruses and falsely predicted 4463 non-viral sequences (Archaea: 1500, Bacteria: 1058, Eukaryotes: 1905) as viruses. While reducing the minimum score-cutoff to 0.75 increases the total number of correctly predicted viral sequences to 3167, it also drastically increases the amount of false predictions to 9944 (Archaea: 3572, Bacteria: 2364, Eukaryotes: 4008). This trend continues with lower minimum score-cutoff to 0.50 (Viruses: 3988, Archaea: 6626, Bacteria: 4417, Eukaryotes: 6678) and 0.25 (Viruses: 4566, Archaea: 9765, Bacteria: 7054, Eukaryotes: 9594).

949 VirSorter2 generates scores between 0 to 1 (computed on both single and double
950 stranded DNA) and reports potential viral sequences where the maximum of the two
951 scores are >= 0.50. With a minimum score cutoff of 0.95, VirSorter2 correctly predicted
952 2367 viral sequences with 1317 non-viral sequences (Archaea: 97, Bacteria: 1191,
953 Eukaryotes: 29) falsely predicted as viruses. Reducing the minimum score cutoff to
954 0.75 increases correctly the predicted viruses to 2798 but increases the falsely
955 predicted non-viral sequences to 2018 (Archaea: 248, Bacteria: 1692, Eukaryotes:
956 78). At the default score cutoff of 0.50, VirSorter2 correctly predicted 3103 viral
957 sequences with 2427 non-viral sequences (Archaea: 382, Bacteria: 1905, Eukaryotes:
958 140) falsely predicted to be viral.

959

960 In comparison, based on the main taxonomy output table, MIUMS accurately predicted
961 2557 viruses with a total of 32 non-viral sequences (Archaea: 0, Bacteria: 32,
962 Eukaryotes: 0) falsely predicted to be viruses. The secondary taxonomy output table
963 shows another 540 viral sequences correctly being predicted as potential viruses with
964 124 non-viral sequences (Archaea: 3, Bacteria: 122, Eukaryote: 0) falsely reported as
965 potential viral sequences. A total of only 13 eukaryotic sequences falsely predicted as
966 archaea, bacteria or viruses (Archaea: 0, bacteria: 12, Viruses: 1).

967

968 **References**

969

970 1. Finn RD, Bateman A, Clements J, Coggill P, Eberhardt RY, Eddy SR, et al.
971 Pfam: the protein families database. *Nucleic Acids Res* 2014; **42**: D222-30.
972 2. Eddy SR. Profile hidden Markov models. *Bioinformatics* . 1998. Oxford
973 University Press. , **14**: 755–763
974 3. Buchfink B, Xie C, Huson DH. Fast and sensitive protein alignment using
975 DIAMOND. *Nat Methods* . 2014. Nature Publishing Group. , **12**: 59–60
976 4. Zhu W, Lomsadze A, Borodovsky M. Ab initio gene identification in
977 metagenomic sequences. *Nucleic Acids Res* 2010; **38**: e132–e132.
978 5. Boratyn GM, Thierry-Mieg J, Thierry-Mieg D, Busby B, Madden TL. Magic-
979 BLAST, an accurate RNA-seq aligner for long and short reads. *BMC*
980 *Bioinformatics* 2019; **20**: 405.

6. Guo J, Bolduc B, Zayed AA, Varsani A, Dominguez-Huerta G, Delmont TO, Pratama AA, Gazitúa MC, Vik D, Sullivan MB, Roux S. VirSorter2: a multi-classifier, expert-guided approach to detect diverse DNA and RNA viruses. *Microbiome*. 2021 Dec; **9**:1-3.
7. Ren J, Song K, Deng C, Ahlgren NA, Fuhrman JA, Li Y, Xie X, Poplin R, Sun F. Identifying viruses from metagenomic data using deep learning. *Quantitative Biology*. 2020 Jan 22:1-4.